New Developments and Challenges in Remote Sensing, Z. Bochenek (ed.)

Investigation of thermal infrared emissivity spectra of mineral and rock samples

M. Danov & D. Petkov
Solar-Terrestrial Influences Laboratory, Bulgarian Academy of Sciences, Acad.G.Bonchev Str., bld. 3, Sofia 1113, Bulgaria

V. Tsanev
Department of Geography, University of Cambridge, Downing Place, Cambridge, CB2 3EN, UK

Keywords: hemispherical emissivity, thermal infrared, rock samples

ABSTRACT: The results of initial laboratory investigation of spectral hemispherical emissivity of several rocks (granite, sandstone, marble, gabbro, anorthosite, etc.) are reported. A radiometric instrumentation was constructed and utilized to measure the hemispherical radiation reflected by the observed object being irradiated by a parallel infrared beam. Measurements were performed with resolution of about 0.2 μm in thermal infrared (TIR) range (8–12 μm).

1 INTRODUCTION

Remote sensing in the infrared diapason of the spectrum is widely utilized for investigation of Earth's surface. Typically the surface of our planet emits electromagnetic radiation in the spectral interval of 3–14 μm but due to the absorption of atmospheric gasses only the intervals 3–5 μm and 8–14 μm (known as atmospheric windows) are suitable for remote sensing purposes. The first window is particularly useful for detection of hot targets as forest fires and geothermal activities, whilst the second one is appropriate for investigation of vegetation, rock and water surfaces.
The energy conservation law for the radiation interacting with a body can be expressed by the equation

$$\alpha(\lambda) + \rho(\lambda) + \tau(\lambda) = 1, \tag{1}$$

where $\alpha(\lambda)$, $\rho(\lambda)$ and $\tau(\lambda)$ are correspondingly absorption, reflectance and transmittance of the body under consideration. Most of the natural objects, including rocks, are opaque and their transmittance satisfies

$$\tau(\lambda) = 0. \tag{2}$$

Hence, for the opaque objects the Eq. (1) is simplified

$$\alpha(\lambda) + \rho(\lambda) = 1. \tag{3}$$

This means that by measuring the hemispherical reflectance $\rho(\lambda)$ of an opaque surface one can evaluate its absorption $\rho(\lambda)$. The latter quantity equals the hemispherical emissivity $\varepsilon(\lambda)$ according to the Kirchoff's law, i.e.

$$\varepsilon(\lambda) = 1 - \rho(\lambda). \tag{4}$$

The aim of the present work is to elaborate a methodology for determination of the spectral hemispherical emissivity of rocks. The methodology is based on the relation (4). Here the hemispherical emissivity is determined by the hemispherical reflectance that can be measured experimentally. An experimental set-up has been build for precise measurement of the hemispherical reflectance of rocks. By means of the created set-up hemispherical emissivities of rock samples of granite, sandstone, marble, gabbro and anorthosite are determined. These rocks are typical for many geographic regions including Bulgaria. Hence, the knowledge of their emissivity is of significant importance for the development of the remote sensing of the forest, vegetations and other natural objects because the mentioned rocks most frequently are situated close to the investigated objects.

2 METHODOLOGY

The developed experimental set-up used for measurement of hemispherical emissivity spectrum of different rocks is presented in Fig. 1. The emission of an infrared (IR) source is collimated by a ZnSe lens. Afterwards it irradiates the investigated sample which is situated in the first focus of the elliptical gold-coated mirror.

The IR radiation is reflected by the investigated sample into a solid angle of 2π steradians, collected by the elliptical mirror (Thiebaud F. and F. K. Kneubuhl, 1983) and

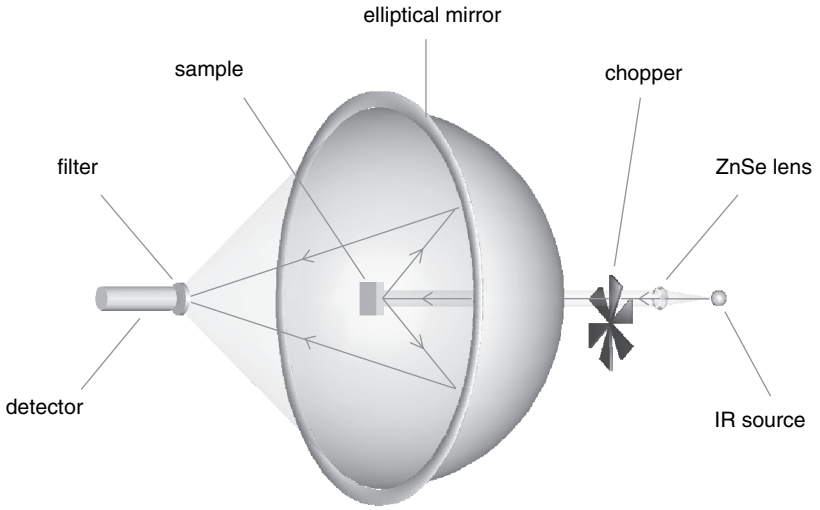

Figure 1. Experimental set-up.

λ_{max}, μm	T_{max}, %	Width at 0.5 T_{max}, μm	Width at 0.1 T_{max}, μm
7.70	50	0.18	0.70
7.86	47	0.18	0.75
8.15	52	0.24	0.74
8.22	54	0.23	0.78
8.55	52	0.22	0.72
8.87	47	0.22	0.75
9.12	54	0.22	0.73
9.22	52	0.22	0.73
9.35	50	0.23	0.68
9.50	49	0.23	0.53
9.90	37	0.24	0.80
10.25	46	0.28	0.83
10.33	43	0.30	0.71

λ_{max}, μm	T_{max}, %	Width at 0. 5 T_{max}, μm	Width at 0.1 T_{max}, μm
10.40	53	0.25	0.80
10.60	55	0.24	0.80
10.70	57	0.25	0.80
10.86	52	0.28	0.92
11.30	37	0.30	1.10
11.70	40	0.28	0.72
11.90	46	0.29	0.76
12.25	41	0.33	0.88
12.30	45	0.28	1.00
12.50	42	0.29	1.00
12.80	39	0.30	1.00
13.15	40	0.29	0.83
13.40	40	0.31	0.84

Table 1

focused onto its second focus where a pyroelectric detector type PLT22 is located. The spectral resolution of the scattered by the sample emission is provided by set of narrow-band transmission filters positioned in front of the detector. The advantage of the developed experimental system is its simplicity.

The used filters are characterized by their maximal transmission T_{max}, determined at the center of the filter transmission profile. The width of the transmission profile at the $0.5T_{max}$ and $0.1T_{max}$ levels is also specified. All three parameters of the used filters are presented in Table 1.

Taking into consideration the data presented in Table 1, the filter profiles are fitted as it is illustrated in Fig. 2 and the transmission areas are determined by proper software.

As it can be seen from Fig. 3 the transmission areas of the different filters differ by factor less than 2. In the presented measurements, the determined transmission area of the filters is used for correction of their integral transmittance.

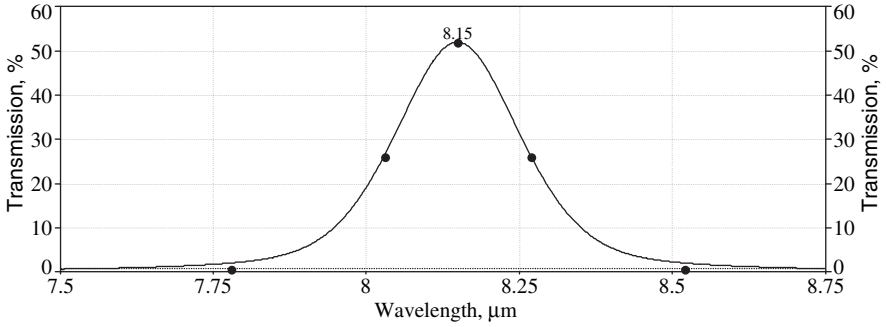

Figure 2. Transmission profile of filter with $\lambda_{max} = 8,15$ μm. Transmissions taken from Table 1 are denoted by points.

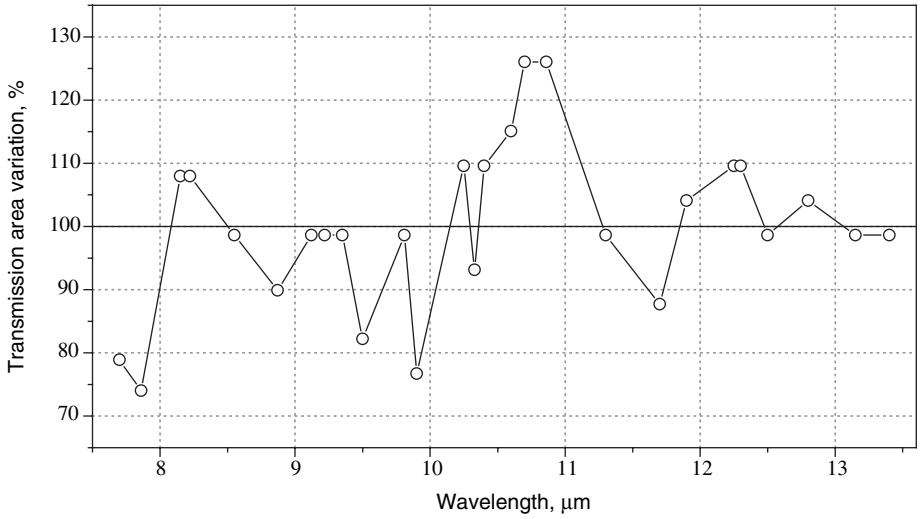

Figure 3. Variation of the transmission area of the filters.

Another part of the experimental set-up that needs characterization is the IR source. In Fig. 4 the spectral profile of the IR source emission is shown. For its measurement the sample is removed and thus the detector registers the intensity of the collimated IR beam. The obtained spectrum dependence is determined by the temperature of the source, which is heated to over 1100°C.

Emissivity spectra determination consists of two stages. The first stage is related to radiometric calibration of the measuring system. For this purpose the sample is replaced by a Lambertian ideal reflection standard–a gold-coated sandpaper of 600 grits per square millimeter. (Stuhlinger *et al*. 1981)

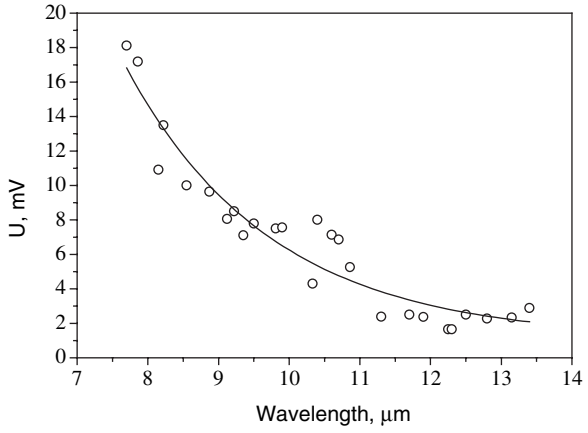

Figure 4. Spectral intensity of the IR source.

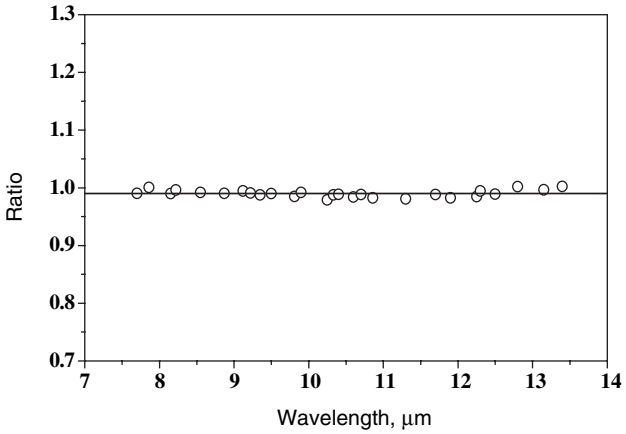

Figure 5. Ratio between the two standards values.

For comparison another standard is prepared from 400-grit sandpaper. To asses the difference of the standards, the ratio between their reflectance values is presented in Fig. 5. The magnitude of the reflected signal is determined by the optical properties of the experimental setup and the spectral response of the PLT22 detector. From Fig. 5 it can be seen that the reflectance of the samples can be measured with the accuracy of ± 0.02.

The second stage is the assessment of the reflectance spectrum of different rock samples. The emissivity of the samples is then evaluated by the following ratio:

$$\varepsilon(\lambda) = U_s(\lambda)/U_R(\lambda), \tag{5}$$

where $U_s(\lambda)$ and $U_R(\lambda)$ are the detector output voltages registered when measuring sample or etalon, respectively.

In order to enhance the signal-to-noise ratio, the IR source radiation was amplitude modulated by chopper at frequency of 8 Hz.

The detector's signal was amplified by a selective amplifier at the same frequency. Thus the influence of the background IR radiation was diminished whilst the signal-to-noise ratio was enhanced. The data registered by the detector were transformed by an analogue-to-digital converter and then processed by a PC.

3 RESULTS AND DISCUSSION

By means of the described methodology the spectral emissivities of samples of some rock and mineral types are determined.

As an example the measured emissivity of granite is presented in Fig. 6. It should be mentioned that the investigated surface of the samples is smooth cut and not treated additionally. The dimensions of the observed side are 2 cm $\times$ 4 cm and the average values of the spectra of five different measurements per sample are obtained.

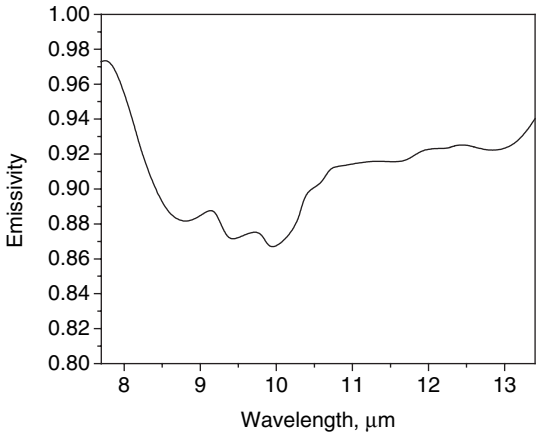

Figure 6. Emissivity of granite.

It can be seen that two well pronounce minima in the emissivity can be distinguished around 8.6 and 9.8 μm. The other features of the measured rock spectrum are below the sensitivity of our measurements. Because of that at this stage of our work we discuss only the two mentioned minima. The reasons for their observation can be related to the mineral structure of granite illustrated in Fig. 7. Granite is a coarse-grained intrusive igneous rock compound of quartz, plagioclase feldspar and potassium feldspar. The emissivity spectra of the forming granite minerals have been found from the literature. Analysis and comparison of the spectra of the forming minerals (Christensen *et al*. 2000, Wendy *et al*. 2005, Johnson *et al*. 2003) with that measured in our experiment show that the typical minima observed in our measurement is caused by the two types of feldspar. During our measurements we have observed similar spectra of anorthosite. Based on the literature study we believe that this similarity is caused by the presence of feldspar in both rocks.

The measured spectrum of limestone emissivity is shown in Fig. 8. A well pronounced minimum around 11, 4 μm can be seen. The limestone is a sedimentary rock

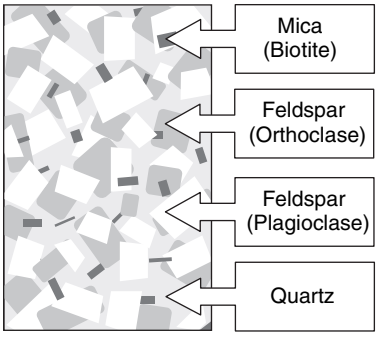

Figure 7. Rock-forming minerals of granite.

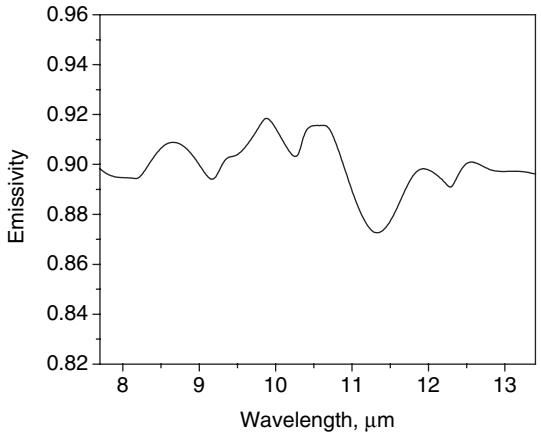

Figure 8. Emissivity of limestone.

composed largely of the mineral calcite (calcium carbonate: $CaCO_3$). Limestones often contain also variable amounts of silica. From the Ref. (Christensen *et al*. 2000) it can be seen that the carbonates exhibit typical minima at 11, 4 μm. Hence, the observed in our measurements reduction in limestone emissivity around 11, 4 μm can be attributed to the calcite.

As a third example, the emissivity spectrum of hematite is illustrated in Fig. 9. It can be seen that the emissivity variations of hematite are less than those observed for the two previous rocks. This can be supported by the Ref.(Glotch *et al.* 2005) where it has been shown that in the 7–14 μm diapason hematite does not show significant variation of its emissivity.

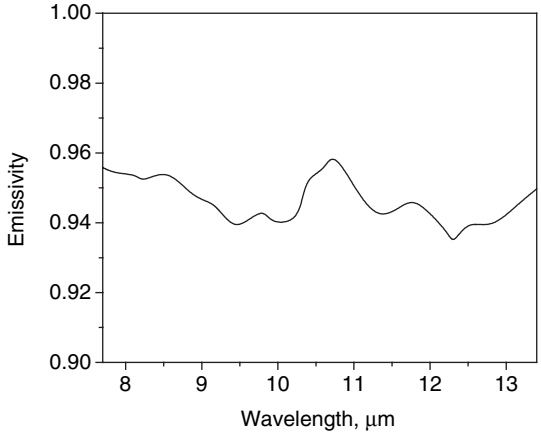

Figure 9. Emissivity of hematite.

5 CONCLUSIONS

A simple experimental set up is built for absolute measurement of the emissivity of objects in the thermal infrared range (8–12 μm) of the spectrum. Based on this set up a methodology is developed for emissivity measurement based on the comparison of the values of reflected by the sample and Lambertian ideal reflection standard radiations. The proposed methodology is illustrated measuring emissivity of rock samples of granite, sandstone, marble, gabbro and anorthosite.

The obtained spectral emissivities will be used for rock identification, when analyzing satellite data and also for evaluation of the atmospheric influence on the remote sensing results.

Another potential application is improvement of algorithms for retrieval of volcanic gas composition based on the absorption spectra registered by Fourier transform IR spectrometers using hot volcanic rocks as source of IR radiation.

ACKNOWLEDGEMENTS

This work is financially supported by Bulgarian Science Fund under contract NZ-MU - 1502/05. The authors express gratitude to Prof. Stefka Cartaleva.

REFERENCES

Christensen Philip R., Joshua L. Bandfield, Victoria E. Hamilton, Douglas A. Howard, Melissa D. Lane, Jennifer L. Piatek, Steven W. Ruff, and William L. S. 2000. A thermal emission spectral library of rock-forming minerals, *Journal of geophysical research*, vol. 105, NO. E4, PAGES 9735–9739, APRIL 25, 2000.

Glotch T.D. , Philip R. Christensen, Thomas G. Sharp 2006. Fresnel modeling of hematite crystal surfaces and application to martian hematite spherules. *Icarus 181 (2006) 408–418.*

Johnson J.R., Friedrich Hörz and Matthew I. St. 2003. Thermal infrared spectroscopy and modeling of experimentally shocked plagioclase feldspars, American Mineralogist, Volume 88, pages 1575–1582.

Stuhlinger T.W., E.L. Dereniak, Bartell F.O. 1981. Bidirectional reflectance distribution function of gold-plated sandpaper, *Applied optics*/Vol.20, No. 15/ 1 August.

Thiebaud F. and F.K. Kneubuhl, Infrared properties of quartz fibres and wool, *Infrared Phys. Vol. 23*, No. 3, pp. 131–148, 1983.

Wendy M. Calvin, Chris Kratt, and James E. Faulds, Infrared spectroscopy for drillhole lithology and mineralogy, Proceedings, *Thirtieth workshop on geothermal reservoir engineering stanford university, stanford*, California, January 31-February 2, 2005 SGP-TR–176.